

# Unusual accelerated molecular relaxations of a tin fluorophosphate glass/polyamide 6 hybrid studied by broadband dielectric spectroscopy

Kevin Urman, Samy Madbouly, Joshua U. Otaigbe\*

*School of Polymers and High Performance Materials, The University of Southern Mississippi, Hattiesburg, MS 39406, USA*

Received 10 October 2006; received in revised form 4 January 2007; accepted 15 January 2007

Available online 24 January 2007

## Abstract

Phosphate glass (Pglass)/polymer hybrids are a relatively new class of materials that combine the advantages of classical polymer blends and composites without their disadvantages. In the case of highly interacting Pglass/polymer (i.e., polyamide 6) hybrids, counter-intuitive properties that are difficult to explain are often observed. To shed light into the origins of the special behavior of the hybrids, we investigated the molecular relaxation processes in the hybrids using broadband dielectric spectroscopy. The dielectric loss spectra were fitted with the Havriliak–Negami equation and the characteristic relaxation times of the hybrid and the pure components were observed. The temperature dependence of the characteristic relaxation times was described using either the Vogel–Fulcher–Tammann, for the  $\alpha$ -relaxations, or an Arrhenius type equation, for the  $\beta$ - and  $\gamma$ -relaxations. The addition of Pglass greatly accelerated both the  $\alpha$ - and  $\beta$ -relaxations of the polyamide 6. However, the  $\gamma$ -relaxation was found to be independent of Pglass composition. This suggests partial miscibility in the solid state, which was confirmed via NMR spectroscopy. The unexpected dramatic change in the  $\beta$ -relaxation process in the 10 vol.% Pglass hybrid suggests that blending can change the local environment of polyamide 6 due to the nanoscale morphology of this system as confirmed by TEM and NMR. It is thought that the fraction of miscible Pglass disrupts the hydrogen bonding between polyamide 6 chains and thereby reduces coordinated, multiple chain motion. In turn, this produces a plasticization effect and possible modification of the polyamide 6's crystalline structure in the Pglass/polyamide 6 hybrids.

© 2007 Elsevier Ltd. All rights reserved.

*Keywords:* Phosphate glass/polyamide 6 hybrid materials; Dielectric spectroscopy; Molecular relaxations

## 1. Introduction

Polymer blends are of great interest to both industrial and academic researchers. The industrial importance of polymer blends stems from the ability to tailor properties to meet specific application needs at a low cost. This makes these materials a more economically viable option as compared to synthesizing a new polymer. From a fundamental science viewpoint, these materials offer a great opportunity to study the effect of interactions on important material parameters such as the glass transition temperatures, melting point, and mechanical properties. Despite the large amount of research

that is being performed on classical polymer blends, they are unable to fulfill the growing need for new advanced materials.

Phosphate glass (Pglass)/polymer hybrids are a relatively new class of materials that are helping to meet the demand for advanced materials. These hybrids combine the advantages of classical polymer blends and composites without their disadvantages. Pglass/polymer hybrids are mixtures of an ultra-low glass transition ( $T_g$ ) Pglass and an organic polymer. Phosphate glasses that display both water resistance and chemical durability are now readily available [1]. One such Pglass is tin fluorophosphate glass which is known to be extremely resistant to water and chemical degradation [2–5]. The low  $T_g$  of the Pglass allows these materials to be melt processed with organic polymers using conventional polymer processing methodologies to yield a hybrid that can contain up to 60 vol.% (i.e., 90 wt.%) of the inorganic component. Because both the organic polymer and the inorganic Pglass are fluids

\* Corresponding author. Tel.: +1 601 266 5596; fax: +1 601 266 5504.

E-mail address: [joshua.otaigbe@usm.edu](mailto:joshua.otaigbe@usm.edu) (J.U. Otaigbe).

during processing, the morphologies of these materials can be controlled, the interactions between components can be tailored, and the intractable viscosity problem inherent to conventional polymer composites at high solid filler (e.g., borosilicate glass) compositions is circumvented [6–8].

Previous work on the behavior and properties of Pglass/polymer hybrids concentrated on either high-end engineering thermoplastics (i.e., PEEK, PEI, etc.) or non-polar commodity resins (PP, PS) [6,9–16]. Recently, this previous work was expanded into highly interacting, polar resins such as polyamide 12 and polyamide 6 [7,17]. It had been previously shown that amines will bind to the surface of phosphate glasses [18]. This classical interaction facilitates a high degree of compatibility between the two phases of the hybrid. Urman and Otaigbe have shown that tin fluorophosphate glass forms a partially miscible phase with polyamide 6 in the melt state via melting point depression [17]. The formation of a partially miscible phase in the melt resulted in special solid-state properties. These materials displayed a 10 °C drop in their  $T_g$  with the addition of 10 vol.% Pglass [17]. This plasticizing effect was also reflected in the tensile mechanical properties of the material which were remarkably similar to that obtained when a plasticizer is added to a pure polymer [17]. It is important to note that the  $T_g$  reduction just mentioned suggests that Pglass is an efficient *inorganic* plasticizer for polyamide 6 and may prove to be a facile and efficient plasticizing method for polyamides and other related engineering plastics, facilitating their processing using conventional polymer processing methods such as extrusion and injection molding. To our knowledge this is the first reported evidence of inorganic plasticizer (that is either a *solid* or *fluid* at ambient and processing temperatures, respectively) for polymers as compared to conventional liquid plasticizers (e.g., low molecular weight liquids such as phthalate esters and various oils) that pervade the literature. Further, the observed effect of the Pglass in the polyamide 6 described in the current article represents the first conclusive evidence of intimate (molecular level) mixing of the hybrid components, suggesting that the Pglass/polyamide 6 system is an excellent model system for exploring new routes for driving organic polymers and inorganic glass to self-assemble into useful organic/inorganic hybrid materials. Therefore, it is likely that increased research attention will be given to this hybrid system in the future by other researchers.

Similar reductions of the  $T_g$  have been observed for several nanocomposite systems [19–21]. Ash et al. found that the addition of <1 wt.% of spherical alumina nanoparticles to poly(methyl methacrylate) caused a  $T_g$  reduction of 25 °C [19,20]. This behavior was conjectured to be the result of the formation of an interaction zone, which is a highly mobile liquid-like area. This region of mobility disrupts the percolation of the slower moving regions and results in a decrease of the  $T_g$  [20]. Similar  $T_g$  reductions were observed for polymers that had polyhedral oligomeric silsesquioxane (POSS) added to the matrix. While the observation of accelerated glass transition relaxations was studied via dynamic mechanical analysis (DMA) in the work just mentioned, it is also possible

to use broadband dielectric relaxation spectroscopy to study the relaxation behavior of these materials.

Dielectric relaxation spectroscopy (DRS) or electrical impedance spectroscopy is used to probe long and short range motions of macromolecular fragments or motions of mobile charges as a function of both signal frequency and temperature. DRS can measure the same thermal relaxations as DMA, but DRS looks at them from a different perspective. DRS can investigate motions over a broader frequency range as well as detect the presence of mobile charges, which is not possible with the DMA technique. However, DRS depends on the presence of dipoles and is therefore less useful for investigations into non-polar polymers. Nonetheless, DRS has been used by many different researchers on many different systems reported in the literature.

Two areas that have greatly benefited from the use of DRS are miscible polymer blends and polymer composites. Several researchers have used DRS to examine the degree of miscibility in polymer blends [22–26]. Peak shifts and broadening are commonly observed for miscible or partially miscible polymer blends. Some researchers have also shown that the strong intermolecular hydrogen bonds present in some miscible blends cause segmental relaxations of the pure components to become coupled and move in concert [27]. However, hydrogen bonding between two organic polymers is not the only factor that can influence the relaxation behavior of the polymers. The addition of inorganic fillers to a polymer matrix also greatly influences the relaxations of the polymer. It has been shown by Perrin et al. that the formation of a nanoscale inorganic sol–gel network causes a broadening of the isochronal dielectric loss curve as well as regions of restricted polymer mobility [28]. Traditional clay/polymer nanocomposites have also been studied via DRS [29,30]. Lee et al. found that exfoliated clay/polyamide 11 nanocomposites greatly accelerated the  $T_g$  ( $\alpha$ -relaxation) of the polymeric component [30]. It was suggested that the clay greatly diminished intermolecular cooperativity, which resulted in an accelerated  $\alpha$ -relaxation.

The origins of the previously mentioned  $T_g$  reduction in Pglass/polyamide 6 hybrids are currently unknown. Because NMR spectroscopy can distinguish between different phases based on conformational and dynamical differences, we will use NMR experiments in future proposed research to provide additional insights into the molecular dynamics and relaxation processes of the hybrid system. The work reported in this article is the first dielectric study of Pglass/polymer hybrids and should provide a solid basis for understanding the effect of Pglass on polymer relaxation behavior.

## 2. Experimental

### 2.1. Materials preparation

The low  $T_g$  tin fluorophosphate glass used in this study has a molar composition of 50% SnF<sub>2</sub> + 20% SnO + 30% P<sub>2</sub>O<sub>5</sub>. The tin fluoride and tin oxide were supplied by Cerac Inc. and the ammonium phosphate was supplied by Sigma–Aldrich. The polyamide 6 used was Capron 8270 HS supplied by Allied

Signal. A hybrid containing 10% Pglass by volume was prepared using a Thermo-Haake Polydrive<sup>®</sup> Melt Mixer equipped with roller blades. The hybrid was mixed at 250 °C with a rotor speed of 75 rpm for testing. The melt-mixed hybrid material was collected in “chunks” from the Polydrive<sup>®</sup>. The “chunks” and pure polyamide 6 were subsequently compression molded into thin films (130 μm thick) at 250 °C using a Tetrahedron<sup>®</sup> compression molder. A thin film (500 μm thick) of the pure Pglass was created by pressing a disk of Pglass between two sheets of release film in a TA Instruments ARES<sup>®</sup> at 250 °C equipped with parallel plate tools. Prior to testing, all the samples were dried in a vacuum oven at 70 °C for at least 24 h or until a constant weight was achieved.

## 2.2. Dielectric relaxation spectroscopy

Spectra were collected using a Novocontrol GmbH Concept 40 Broadband Dielectric Spectrometer with an Alpha A analyzer over the frequency range of 0.01 Hz to 1 MHz. The range of tested temperatures, within  $\pm 0.2$  °C, was  $-120$  °C to  $150$  °C in increments of  $10$  °C. Samples of the hybrid and pure polyamide 6 were punched into circular disks (25.4 mm in diameter) from the compression molded films previously described. The method for pressing the pure Pglass samples resulted in a circular disk with a nominal diameter of 25 mm. The samples were sandwiched between two 20 mm gold plated electrodes. There was an ‘overhang’ of the samples to adjust for the fringing fields around the edge of the electrodes that become more important as the sample becomes thicker. Running the samples in this manner reduces the error by forcing the fringe fields, while not being uniform, to at least pass through the sample.

## 2.3. Transmission electron microscopy

Samples for transmission electron microscopy (TEM) were prepared by taking a small portion of the hybrid material (approximately  $0.5$  mm  $\times$   $0.5$  mm) and affixing it onto either a stub or pin holder. The material was frozen to  $-100$  °C and ultra-thin sections were made using a Meager Scientific Reichert Ultracut S<sup>®</sup> ultramicrotome with a FCS cryo-unit and a diatome diamond knife. The sections were collected onto formvar coated copper grids using cryoprotectant solution with a wire loop. The cryoprotectant was removed from the sections with distilled water. The grids were then exposed to 0.5% ruthenium tetroxide (RuO<sub>4</sub>) in solution by affixing the grids with tape in a glass Petri dish and suspending them over a droplet of the RuO<sub>4</sub> for 2 h. The grids were then imaged using a JEOL 1200 EX II<sup>®</sup> transmission electron microscope at 120 kV. Images were collected using a Megaview III camera and SIS Pro software.

## 3. Results and discussion

Fig. 1 is an isochronal graph of the dielectric loss of the pure components and the hybrid (10 vol.% Pglass) as a function of temperature. Three relaxations can be identified in

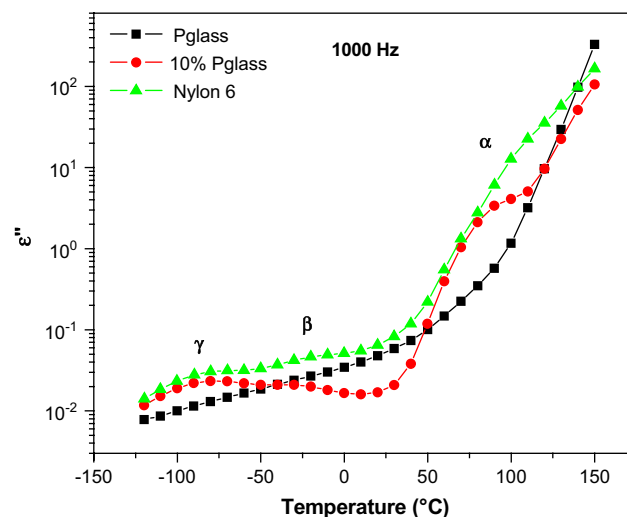


Fig. 1. Temperature dependence of the dielectric loss for the pure components and the hybrid at 1000 Hz.

both the hybrid and the pure polyamide 6. These relaxations have been identified and reported for the pure polyamide 6 [31–34]. The low temperature  $\gamma$ -relaxation involves the motion of very short  $-\text{CH}_2$  segments and an amide group which provides the dielectric activity. Assignment of the molecular motions associated with the mid-temperature range relaxation (i.e.,  $\beta$ -relaxation) is relatively more complicated and a number of varying opinions exist in the literature. Frank et al. attribute the  $\beta$ -relaxation to the movement of more extended  $-\text{CH}_2$  segments as well as motions of the amide groups [31]. These motions are exacerbated by the presence of water in the system. Laredo et al. believe that the  $\beta$ -relaxation is due solely to firmly bound water that is often present in polyamides despite drying and can be completely eliminated only by extremely rigorous drying procedures [32]. In the review by McCrum and Williams, the dielectric  $\beta$ -relaxation was attributed to  $-\text{NH}_2$  and  $-\text{OH}$  chain end group movements by some groups, while others attributed it to the motion of a water-polymer complex [34]. In the present work, the effect of water on the  $\beta$ -relaxation is considered to be negligible due to the initial drying procedure that was performed on the materials prior to testing. If any small amount of water remained in the materials, it was firmly bound water. Additionally, similar amounts of bound water should be present in all tested samples, thereby making direct comparison of results possible. The  $\alpha$ -relaxation (the highest temperature relaxation) is connected with the onset of large-scale motions of the chain segments in the vicinity of the  $T_g$ . The pure Pglass only displays a single relaxation, which is not seen in the isochronal graph (Fig. 1) due to the high conductivity of the pure Pglass at elevated temperatures. The 10 vol.% Pglass hybrid also displays an increase in permittivity at elevated temperatures, but this should not be confused with its  $\alpha$ -relaxation process, which is clearly evidenced by the peak at approximately  $75$  °C. However, this process can be clearly seen in isothermal graphs, as will be discussed later. This relaxation in the pure Pglass, which we label as the  $\alpha$ -relaxation, is similar to the dipole losses observed for polymers, but is most likely due

to separated ion pairs [35]. From Fig. 1, it is easily observed that the hybrid's  $\alpha$ -relaxation occurs at a lower temperature than either of the pure components, indicating a physiochemical interaction between the hybrid components. Further, the hybrid displays a single  $\alpha$ -relaxation which seems to indicate that the Pglass domains are not large enough to contribute to the appearance of a fourth relaxation in the hybrid. The appearance of a single  $T_g$  is often used as a criteria for miscibility in classical polymer blend systems, where the blend  $T_g$  is typically between the pure components [36–39].

While the appearance of a single  $T_g$  in the hybrid suggests at least partial miscibility, the temperature reduction of the  $T_g$  is not explained in the miscible polymer blend literature. Similarly, the  $\beta$ -relaxation of the hybrid appears at a reduced temperature when compared to that of the pure polyamide 6. However, the  $\gamma$ -relaxation remains relatively unaffected. These effects are more clearly observed in isothermal curves shown in Fig. 2. These experimental results depicted in Fig. 2 suggest that the local environment of polyamide 6 changes by blending due to the nanoscale morphology of this system, which will be discussed later. Fig. 2 displays the dielectric loss as a function of frequency at  $-40^\circ\text{C}$  for the pure polyamide 6 and the 10 vol.% Pglass hybrid. The pure Pglass was omitted from this figure because it shows no relaxation at this temperature. Although the  $\gamma$ -relaxations of the pure polyamide 6 and the hybrid are almost identical, the  $\beta$ -relaxation of the hybrid has shifted to a much higher frequency and has almost become a shoulder in the hybrid's  $\gamma$ -relaxation. In Fig. 3, the dielectric constant and loss as a function of frequency are shown for both the pure components and the hybrid at the higher temperature of  $80^\circ\text{C}$ , which is in the range of the  $\alpha$ -relaxation process. From the dielectric loss measurements at this temperature, one can see that the polyamide 6 shows a  $\beta$ -relaxation process with a maximum frequency ( $f_{\text{max}}$ ) of about  $3 \times 10^5$  Hz. In addition, the  $\alpha$ -relaxation process of the polyamide 6 appears with an  $f_{\text{max}}$

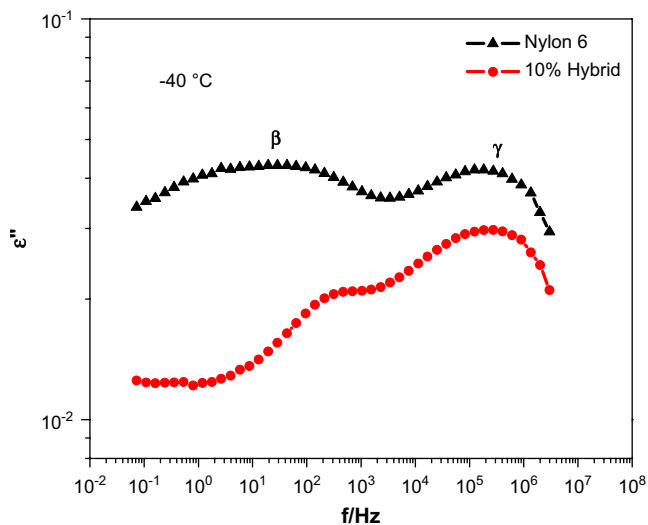


Fig. 2. Dielectric loss as a function of frequency at  $-40^\circ\text{C}$ . Note that the Pglass data are omitted because it displays no relaxation at this temperature.

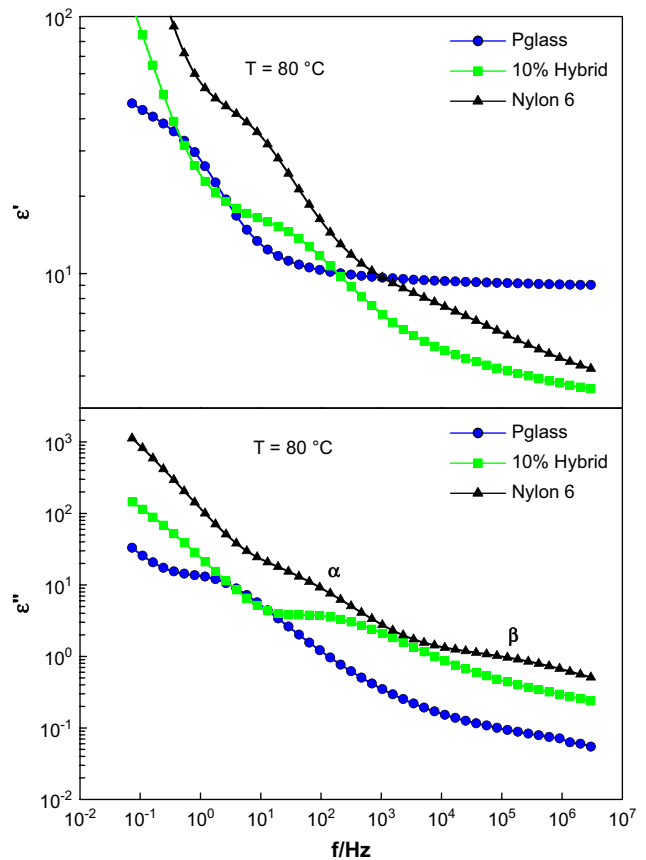


Fig. 3. Dielectric constant and loss as a function of frequency at  $80^\circ\text{C}$  for the pure components and the hybrid.

of around  $10^2$  Hz. For the Pglass, the  $\alpha$ -relaxation appears at an  $f_{\text{max}}$  of 5 Hz. On the other hand, only one relaxation process, the  $\alpha$ -relaxation, is observed for the hybrid at  $f_{\text{max}} \approx 7 \times 10^2$  Hz. The  $\beta$ -relaxation process of the hybrid has shifted to a higher frequency that is outside the range of the measurement. Further, it is noteworthy that the observed height of the  $\alpha$ -relaxation process in the hybrid is below that of either of the pure components. The dispersion region of  $\epsilon'$  occurs at the same frequency range of the peak maximum of  $\epsilon''$ . The magnitude of  $\epsilon'$  increases at the low frequency range due to the contribution of the ionic conductivity.

It is possible to model these relaxations using the well known phenomenological Havriliak–Negami (HN) equation with an added ionic conductivity term (Eq. (1)) [34,40–42].

$$\epsilon^*(\omega) = \epsilon' - i\epsilon'' = -i \left( \frac{\sigma_0}{\epsilon_0 \omega} \right) + \sum_{k=1}^3 \left[ \frac{\Delta\epsilon_k}{(1 + (i\omega\tau_k)^{a_k})^{b_k}} + \epsilon_{\infty k} \right] \quad (1)$$

In this equation,  $\epsilon^*$  is the complex dielectric constant. The energy storage per cycle and the energy loss or absorption per cycle are represented by  $\epsilon'$  and  $\epsilon''$ , respectively.  $\sigma_0$  is the dc conductivity,  $\epsilon_0$  is the permittivity of free space (8.854 pF/m),  $\omega$  is the angular frequency, and  $i$  is equivalent to  $-1^{1/2}$ .  $\Delta\epsilon_k$  is the strength of the  $k$ th relaxation,  $\epsilon_{\infty k}$  is the high frequency relative permittivity of the  $k$ th relaxation,

and  $\tau_k$  is the characteristic relaxation time of the  $k$ th component. The exponents  $a$  and  $b$  are distribution parameters that describe the symmetric and asymmetric broadening of the relaxation time distribution function, respectively. When  $a = 1$ , the HN equation reduces to the Davidson–Cole expression and when  $b = 1$ , the Cole–Cole function is obtained. In the special case of  $a$  and  $b$  both being equal to unity, the Debye equation is obtained. Fig. 4 displays the fitting that is obtained when two HN terms are used to fit relaxation spectrum obtained for the hybrid at 70 °C. The fit is quite good and the characteristic relaxation time for each relaxation process can be extracted. The figure can be resolved into  $\alpha$ -,  $\beta$ -relaxation processes and ionic conductivity as shown by the dotted lines. Note that the solid line passing through the experimental data points represents the sum of the three processes. Table 1 displays the fit parameters of the HN equation to the  $\alpha$ -relaxation of the pure Pglass, pure polyamide 6, and the hybrid at 80 °C (i.e., fits to data of Fig. 2b). The distribution parameters fall within acceptable limits, but the more interesting information is contained in the dielectric strength ( $\Delta\epsilon$ ) of each material's  $\alpha$ -relaxation. The value of  $\Delta\epsilon$  of the hybrid is considerably lower than that of both pure polyamide 6 and pure Pglass. This behavior suggests that the number of reoriented dipoles decreases significantly in the hybrid compared to the pure components. Similar behavior is observed for the  $\beta$ -relaxation of the hybrid and pure polyamide 6. The decrease of  $\Delta\epsilon$  may be attributed to possible Pglass-induced crystallinity and formation of new crystal modification in the polyamide 6 as confirmed by NMR data that will be reported in the second paper to be published elsewhere. This crystal modification is due to the very fine morphology of the dispersed Pglass in the polyamide 6 matrix, which can act as a nucleating agent for the crystallization process as discussed later [43]. Therefore, the segmental motions are highly constrained by the increase in the crystalline regime of the hybrid.

This hypothesis just mentioned is consistent with previously reported  $^1\text{H}$ – $^{31}\text{P}$  solid state and  $^{31}\text{P}$  [43] heteronuclear recoupling with dephasing by strong homonuclear interactions of protons' (HARDSHIP) NMR data on the Pglass/polyamide

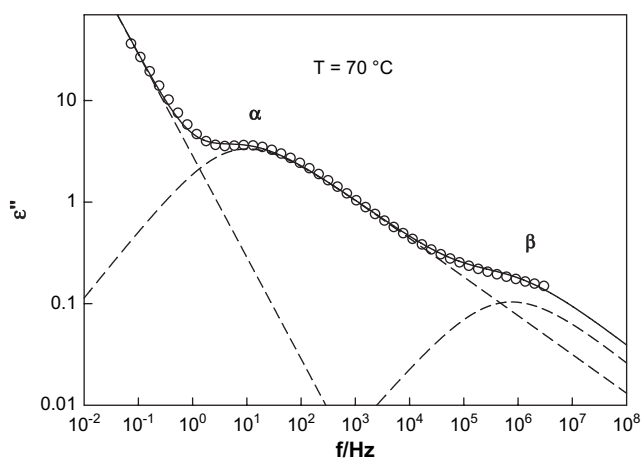


Fig. 4. Havriliak–Negami fit of the dielectric loss spectrum of the 10 vol.% Pglass/polyamide 6 hybrid at 70 °C.

Table 1  
Fit parameters of the HN equation of the  $\alpha$ -relaxation at 80 °C

Vol.% Pglass	$a$	$b$	$\Delta\epsilon$
0	0.8489	0.6162	25.58
10	1	0.3239	11.02
100	0.8506	1	15.17

6 hybrid [43]. The NMR data revealed that  $^1\text{H}$  spin diffusion from 75% of the  $^1\text{H}$  in the glass to the polyamide is within 50 ms, indicating proximity on a 30 nm scale. Fast dephasing of a quarter of the  $^{31}\text{P}$  magnetization by dipolar couplings to polyamide protons in  $^{31}\text{P}$  [43] HARDSHIP NMR showed that 25% of the Pglass is within 0.5 nm from the polyamide. This is confirmed by  $^1\text{H}$ – $^{31}\text{P}$  heteronuclear correlation NMR spectra with inverse  $T_{2,H}$  filtering, which showed relatively fast (1 ms) cross-polarization from PA6 protons, identified by their upfield chemical shift and short transverse relaxation time  $T_{2,H}$ , to a significant fraction of  $^{31}\text{P}$  in the glass [43]. The  $^{31}\text{P}$  spectrum associated with the polyamide  $^1\text{H}$  revealed that the phosphate sites near the polyamide matrix were chemically altered but differently than previously observed in Pglass–polyethylene hybrids, where no such contact was proven. As expected, the  $^{31}\text{P}$  sites that cross-polarize from the polyamide protons also exhibited pronounced dephasing in  $^{31}\text{P}$  [43] HARDSHIP experiments. Additional HARDSHIP experiments after cross-polarization and  $^{31}\text{P}$  spin diffusion experiments indicated that the 25% of phosphate that is within 0.5 nm from the polyamide was not dispersed in the polymer but on the surface of 10 nm diameter Pglass particles. Additional details of this first conclusive NMR evidence of intimate mixing of the hybrid components are available elsewhere [43]. Further, the current study and the previously reported extended NMR study suggest that the Pglass/polyamide 6 system is an excellent model system for exploring new routes for driving organic polymers and inorganic glass to self-assemble into useful organic/inorganic hybrid materials.

The temperature dependence of the characteristic relaxation times of the  $T_g$ -like relaxations (i.e.,  $\alpha$ -relaxations) can then be described using the Volger–Fulcher–Tammann (VFT) equation (Eq. (2)) [44].

$$\tau(T) = \tau_0 \exp\left(\frac{E_a}{k_B(T - T_V)}\right) \quad (2)$$

In the VFT equation,  $k_B$  is the Boltzmann constant,  $E_a$  is an apparent (temperature-dependent) activation energy,  $T_V$  is a hypothetical temperature at which segmental motions are frozen-in, and  $\tau_0$  is a hypothetical relaxation time at infinite temperature. Fig. 5 displays the characteristic relaxation time as a function of inverse temperature. The solid lines represent fits of the data to the VFT equation and Table 2 displays the fitting parameters. Clearly, the figure shows that addition of Pglass to the polyamide 6 accelerates the  $\alpha$ -relaxation of the polymer chains. In turn, the hybrid displays a lower apparent activation energy as compared to that of the pure components. Reduction of a polymer blend's  $T_g$  and its apparent

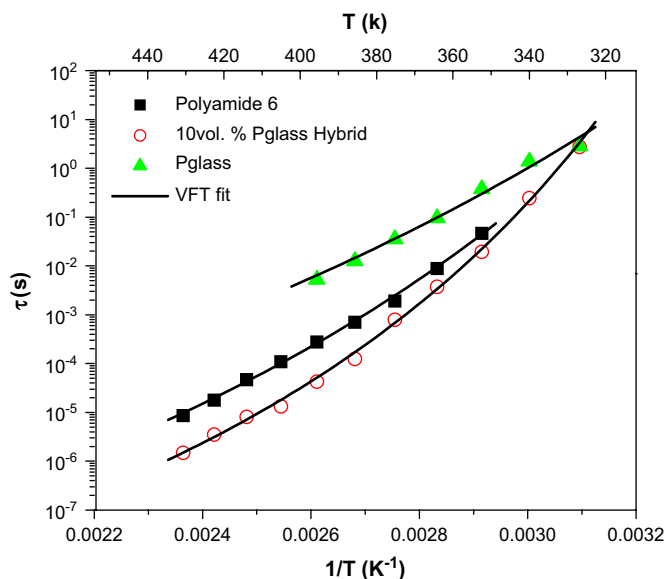


Fig. 5. The characteristic relaxation times of the pure components and hybrid as a function of temperature (solid lines represent fits of the VFT equation).

activation energy are often attributed to partial miscibility of the pure components [25,26]. A similar mechanism is considered to be at work in the present hybrid system. While  $\alpha$ -relaxations are due to long chain motions, the  $\beta$ - and  $\gamma$ -relaxations are due to relatively shorter chain motions. The temperature dependence of these latter relaxations can be modeled by an Arrhenius type expression (Eq. (3)) [45].

$$\tau(T) = \tau_0 \exp\left(\frac{E_a}{k_B T}\right) \quad (3)$$

The variables in Eq. (3) are the same as those in the VFT equation. In Fig. 6, the temperature dependence of the  $\beta$ - and  $\gamma$ -relaxation times of the polyamide 6 and the hybrid is shown. The solid lines are fits of the Arrhenius equation to the data. The activation energy and relaxation time of the  $\gamma$ -process are very similar for both the polyamide 6 and the hybrid as shown in Table 3. The addition of Pglass to the polymer matrix does not affect the very local motions of the  $\gamma$ -relaxation. However, Pglass does affect the  $\beta$ -relaxation in a similar manner to that observed for the  $\alpha$ -relaxation already discussed. Pglass seems to accelerate the motions of long chain segments, but it is unable to significantly impact very short (approximately two  $-\text{CH}_2$  units) motions.

The origin of the observed behavior is believed to be due to the partial miscibility of the pure components in the solid state. While previously reported experimental evidence has

Table 2  
Fit parameters of the VFT equation

	Pglass	Hybrid	Polyamide 6
$\tau_0$ (s)	$4.003 \times 10^{-10}$	$2.201 \times 10^{-12}$	$3.194 \times 10^{-12}$
$E_a$ (eV)	0.3040	0.2218	0.2853
$T_0$ (K)	170.4	231.3	201.3

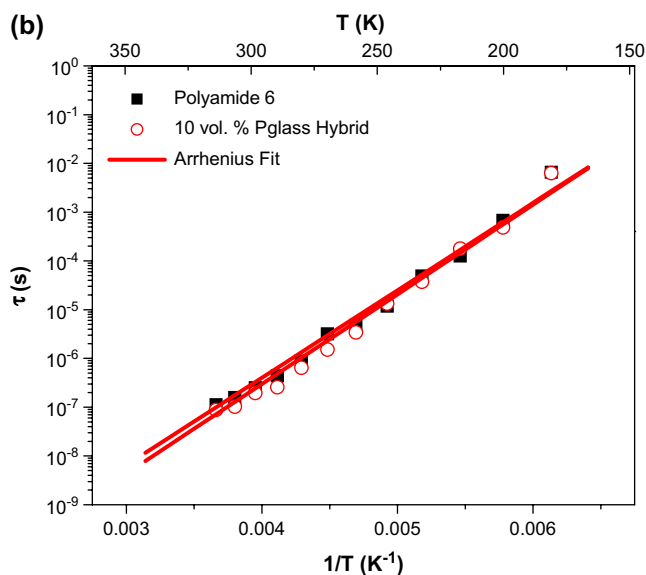
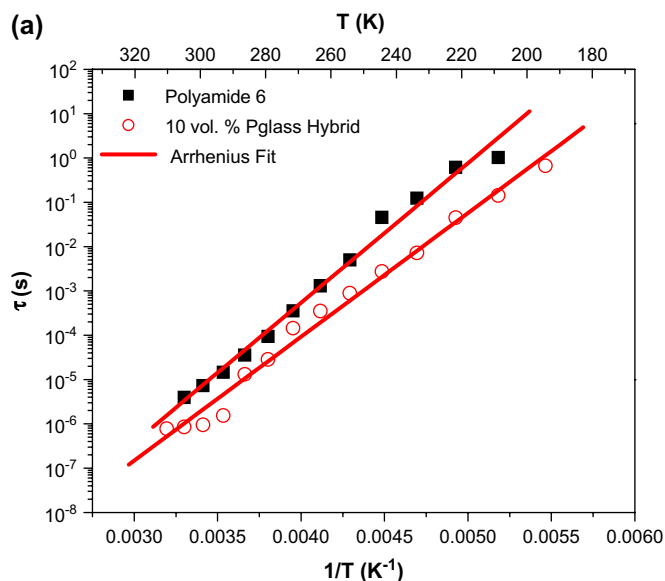


Fig. 6. Temperature dependence of the  $\beta$ - (a) and  $\gamma$ -relaxations (b) of the pure polyamide 6 and the hybrid (solid lines are fits of the Arrhenius equation).

shown that polyamide 6 and Pglass are miscible in the liquid (melt) state, the DRS investigations performed on these materials suggest partial miscibility in the solid state. TEM investigations of the hybrid material display a two-phase microstructure with the Pglass being distributed as droplets in the polymer matrix (Fig. 7). Size analysis of the micrograph reveals an average particle size of  $530 \pm 5$  nm, with the smallest observed particle being  $70 \pm 2$  nm in size. The TEM also

Table 3  
Fit parameters of the Arrhenius equation

	Polyamide 6		Hybrid	
	$\beta$	$\gamma$	$\beta$	$\gamma$
$\tau_0$ (s)	$1.333 \times 10^{-16}$	$2.682 \times 10^{-14}$	$6.117 \times 10^{-16}$	$1.316 \times 10^{-14}$
$E_a$ (eV)	0.2716	0.1546	0.2408	0.1585

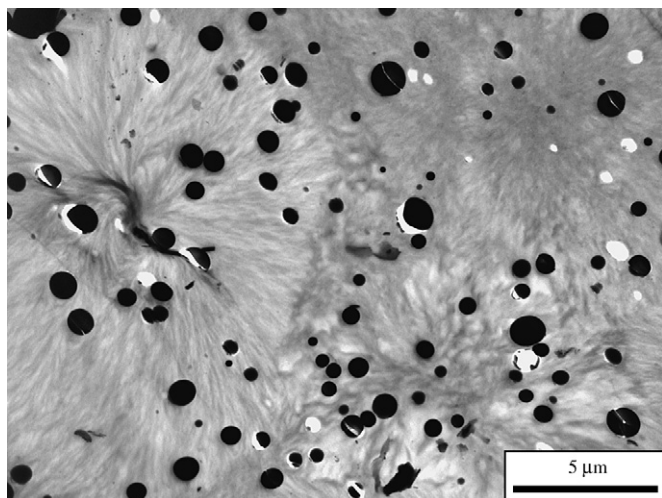


Fig. 7. TEM micrograph of the 10 vol.% Pglass/polyamide 6 hybrid.

shows the spherulites (lamella) of the crystalline structure of the polyamide 6 matrix.

While TEM can observe nanoscale particles, NMR has been shown to be even better suited to estimate the size and amount of Pglass that is distributed within a few nanometers (i.e., the molecular level) of polyamide 6 chains. In a detailed NMR investigation of this material covered in another article reported elsewhere, the HARSHIP method [46] was used successfully to investigate the partial miscibility of the polyamide 6 and the Pglass [43]. The strongly distance-dependent dipolar couplings of the  $^1\text{H}$  nuclear magnets in polyamide 6 dephase the  $^{31}\text{P}$  in the Pglass, while the effects of  $^1\text{H}$  inside the Pglass are removed based on their long transverse ( $T_{2,\text{H}}$ ) relaxation times [46]. As desired, little HARSHIP dephasing was observed in the pure Pglass, while in the hybrid material, quantitative  $^1\text{H}$ – $^{31}\text{P}$  HARSHIP shows fast initial dephasing by the polyamide protons, indicative of 25% of phosphates in intimate contact with the polyamide 6 matrix (data not shown, but available elsewhere [43]). The plateau of 75% shows that the amount of Pglass within 0.5 nm from the polyamide matrix is 25% of the total.

#### 4. Conclusions

Inorganic phosphate glass/organic polymer hybrids are a unique class of materials that display a number of interesting and desirable properties. In the case of highly interacting Pglass/polymer (i.e., polyamide 6) hybrids, the origin of the hybrid's often counter-intuitive properties was previously unknown. While it has been established that Pglass is melt miscible with polyamide 6, the underlying cause of the apparent plasticization effect on the polymer component in the solid state was unknown. Through the application of dielectric spectroscopy and previously reported advanced NMR techniques the partial miscibility of the hybrid components was established. The dielectric loss spectra were fitted with the Havriliak–Negami and the characteristic relaxation times of the hybrid and the pure components were established. The

temperature dependence of the characteristic relaxation times was described using the Vogel–Fulcher–Tammann equation, in the case of the  $\alpha$ -relaxation process, and an Arrhenius type equation, in the case of the  $\beta$ - and  $\gamma$ -relaxations. It was found that the addition of Pglass greatly accelerated both the  $\alpha$ - and  $\beta$ -relaxations of the polyamide 6, while the  $\gamma$ -relaxation was largely unaffected. This behavior qualitatively suggests partial miscibility in the solid state. As previously reported elsewhere [43], we quantitatively determined that a significant fraction of the Pglass was in very close (i.e., 0.7 nm) contact with the polyamide 6 chains, thereby supporting our suggestion for the change of the local environment of the polyamide 6 by blending and why the  $\beta$ -relaxation process is strongly accelerated. The nanoscale Pglass domains may also modify the crystalline structure of the polyamide 6 and affect motions of the polymer chains. We conjecture that the fraction of miscible Pglass disrupts the hydrogen bonding between polyamide 6 chains and thereby reduces coordinated, multiple chain motions. In turn, this produces an unusual plasticization or viscosity decrease effect that is akin to that reported by Mackay and coworkers [47] for a polymer melt filled with nanoparticles. We will use complementary NMR spectroscopy experiments in future proposed research to characterize effects of polymer crystallinity and other molecular-level effects in the hybrids that are responsible for the various relaxation processes reported in the present article.

#### Acknowledgements

We would like to thank the U.S. National Science Foundation Division of Materials Research (grant numbers #97-33350 and #03-09115) for funding and K.U. thanks the Hearin Foundation for fellowship support. We are also grateful to Prof. Klaus Schmidt-Rohr and A. Rawal whose contributions and suggestions resulted in a considerably improved and clearer paper. The assistance of Dr. James Kopchick and Dr. K.A. Mautz in the acquisition of the DRS data is gratefully acknowledged. Prior work of J.U.O.'s former graduate students and collaborators is acknowledged.

#### References

- [1] Brow RK. In: Brow RK, editor. Review: the structure of simple phosphate glasses. Danvers, MA: Elsevier; 1999.
- [2] Tick PA. U.S. Patent 4 379 070 (assigned to Corning, Inc.), 1983.
- [3] Tick PA. *Physics and Chemistry of Glasses* 1984;25(6):149–54.
- [4] Xu XJ, Day DE. *Physics and Chemistry of Glasses* 1990;31(5):183–7.
- [5] Xu XJ, Day DE, Brow RK. *Physics and Chemistry of Glasses* 1995; 36(6):264–71.
- [6] Adalja SB, Otaigbe JU. *Polymer Composites* 2002;23(2):171–81.
- [7] Urman K, Iverson D, Otaigbe JU. *Journal of Applied Polymer Science*, in press.
- [8] Urman K, Schweizer T, Otaigbe J. Uniaxial elongation flow effects and morphology development in LDPE/phosphate glass hybrids. *Rheologica Acta*, submitted for publication.
- [9] Adalja SB, Otaigbe JU, Thalacker J. *Polymer Engineering and Science* 2001;41(6):1055–67.
- [10] Guschl P, Otaigbe JU. *Journal of Colloid and Interface Science* 2003;266: 82–91.

- [11] Guschl P, Otaigbe JU, Loong C-K. *Polymer Engineering and Science* 2004;44(9):1692–701.
- [12] Guschl PC, Otaigbe JU. *Journal of Applied Polymer Science* 2003; 90(12):3445–56.
- [13] Otaigbe JU, Beall GH. *Trends in Polymer Science* 1997;5(11):369–79.
- [14] Otaigbe JU, Quinn CJ, Beall GH. *Polymer Composites* 1998;19(1): 18–22.
- [15] Quinn CJ, Frayer P, Beall G. In: Salamone JC, editor. *Glass–polymer melt blends*. New York: CRC Press; 1996. p. 2766–77.
- [16] Young RT, McLeod MA, Baird DG. *Polymer Composites* 2000;21(6): 900–17.
- [17] Urman K, Otaigbe JU. Novel phosphate glass/polyamide 6 hybrids. *Journal of Polymer Science, Part B: Polymer Physics* 2006;44:441–50.
- [18] Hersh LS, Onyiriuka EC, Hertl W. *Journal of Materials Research* 1995; 10(8):2120–7.
- [19] Ash BJ, Siegel RW, Schadler LS. *Macromolecules* 2004;37:1358–69.
- [20] Ash BJ, Siegel RW, Schadler LS. *Journal of Polymer Science, Part B: Polymer Physics* 2004;42:4371–83.
- [21] Li GZ, Cho H, Wang L, Toghiani H, Pittman Jr CU. *Journal of Polymer Science, Part A: Polymer Chemistry* 2005;43(2):355–72.
- [22] Alegria A, Colmenero J, Ngai KL, Roland CM. *Macromolecules* 1994; 27:4486–92.
- [23] Alvarez F, Alegria A, Colmenero J. *Macromolecules* 1997;30:597–604.
- [24] Dionisio MCS, Ramos JJM, Fernandes AC. *Journal of Applied Polymer Science* 1996;60:903–9.
- [25] Madbouly SA, Otaigbe JU, Hassan MK, Mauritz KA. *Polymer Preprints (American Chemical Society, Division Polymer Materials Science Engineering)* 2006;831–2.
- [26] Pratt GJ, Smith MJA. *Polymer International* 1997;43:137–42.
- [27] Zhang S, Painter PC, Runt J. *Macromolecules* 2002;35:9403–13.
- [28] Perrin FX, Nguyen VN, Vernet JL. *Macromolecular Chemistry and Physics* 2005;206:1439–47.
- [29] Davis RD, Bur AJ, McBrearty M, Lee Y-H, Gilman JW, Start PR. *Polymer* 2004;45:6487–93.
- [30] Lee Y-H, Bur AJ, Roth SC, Start PR. *Macromolecules* 2005;38:3828–37.
- [31] Frank B, Frubing P, Pissis P. *Journal of Polymer Science, Part B: Polymer Physics* 1996;34:1853–60.
- [32] Laredo E, Grimau M, Sanchez F, Bello A. *Macromolecules* 2003;36: 9840–50.
- [33] Laredo E, Hernandez MC. *Journal of Polymer Science, Part B: Polymer Physics* 1997;35:2879–88.
- [34] McCrum NG, Read BE, Williams G. *Anelastic and dielectric effects in polymeric solids*. New York: Dover; 1991.
- [35] O'Reilly JM, Papadopoulos K. *Journal of Materials Science* 2001;36: 1595–600.
- [36] Balsamo V, Calzadilla N, Mora G, Muller AJ. *Journal of Polymer Science, Part B: Polymer Physics* 2001;39:771–85.
- [37] Eguiburu JL, Iruiñ JJ, Fernandez-Berridi MJ, San Roman J. *Polymer* 1998;39(26):6891–6.
- [38] Liu Y, Donovan JA. *Polymer* 1995;36(25):4797–803.
- [39] Zhang SH, Jin X, Painter PC, Runt J. *Polymer* 2004;45:3933–42.
- [40] Havriliak S, Negami S. *Journal of Polymer Science, Polymer Symposia* 1966;14:161–210.
- [41] Kryitsis A, Pissis P, Grigorieva OP, Sergeeva LM, Brouko AA, Zimich ON, et al. *Journal of Applied Polymer Science* 1999;73:385–97.
- [42] Shafee EE. *European Polymer Journal* 2001;37:451–8.
- [43] Rawal A, Urman K, Otaigbe JU, Schmidt-Rohr K. *Chemistry of Materials* 2006;18:6333–8.
- [44] Runt JP, Fitzgerald JJ, editors. *Dielectric spectroscopy of polymeric materials*. Washington, D.C.: American Chemical Society; 1997.
- [45] Laredo E, Grimau M, Bello A, Sanchez F, Gomez MA, Marco C, et al. *Journal of Polymer Science, Part B: Polymer Physics* 2005;43: 1408–20.
- [46] Schmidt-Rohr K, Rawal A, Fang X-W. *Journal of Chemical Physics*, in press.
- [47] Mackay ME, Doa TT, Tuteja A, Ho DL, Van Horn B, Kim HC, et al. *Nature Materials* 2003;2:762–6; See also: Tuteja A, Mackay ME, Kim HC, Hawker CJ, Van Horn B. *Macromolecules* 2005;38:8000–11.